

Supporting information

N-Confused Porphyrin-based Conjugated Microporous Polymers

Qichuan He,^{ab} Jialing Kang,^b Jinhui Zhu,^{*b} Senhe Huang,^{bd} Chenbao Lu,^b Haiwei Liang,^c
Yuezeng Su^{*a} and Xiaodong Zhuang^{*b}

^a *School of Electronic Information and Electrical Engineering, Shanghai Jiao Tong University, Shanghai 200240, China*

^b *The meso-Entropy Matter Lab, State Key Laboratory of Metal Matrix Composites, School of Chemistry and Chemical Engineering, Frontiers Science Center for Transformative Molecules, Shanghai Jiao Tong University, Shanghai 200240, China.*

^c *Hefei National Laboratory for Physical Sciences at the Microscale, School of Chemistry and Materials Sciences, University of Science and Technology of China, Hefei, China*

^d *College of Chemistry, Zhengzhou University, Zhengzhou, Henan 450001, China.*

1. Experiment section

1.1 Materials and methods

4-Bromobenzaldehyde, pyrrole, PtCl_2 , benzonitrile, sodium propionate, 1,5-cyclooctadiene, bis(1,5-cyclooctadiene) nickel, 2,3-dichloro-5,6-dicyano-1,4-benzoquinone, methanesulfonic acid and nitrobenzene were purchased from Sinopharm Chemical Reagent. Chlorobenzene, acetonitrile, 1,2-dichlorobenzene, 2,2'-dipyridyl, acetic acid and methanol were purchased from Sigma-Aldrich.

1.2 Equipment and measurements

Nuclear magnetic resonance (NMR) spectroscopy was tested on Advance III HD 500 of Brooke company with the deuterated reagent of CDCl_3 . The MALDI-TOF mass spectrum was acquired on a AB Sciex 4800 MALDI-TOF mass spectrum equipped with a Nd:YAG laser operating at 355 nm. Scanning electron microscopy (SEM) was performed on a FEI Sirion-200 field emission scanning electron microscope. Transmission electron microscopy (TEM) images were acquired using a Tecnai G2 F20 S-TWIN transmission electron microscope operated at 200 kV. Aberration-corrected high-angle annular dark-field scanning transmission electron microscopy (HAADF-STEM) was performed on Titan Cubed Themis G2 300 (FEI). X-ray diffraction (XRD) analysis was performed on a RigakuD/Max 2500 X-ray diffractometer of $\text{Cu K}\alpha$ radiation ($k = 1.54 \text{ \AA}$) with a scan rate of 6° min^{-1} over the range of $10\text{--}80^\circ (2\theta)$. Fourier transform infrared (FTIR) spectra were recorded on a PerkinElmer Spectrum 100 FTIR spectrometer (UK). The Raman spectroscopy was measured on Lab-RAM HR800 by an argon ion laser of 532 nm. X-ray photoelectron spectroscopy (XPS) was performed on PHI-5000C ESCA system; the C 1s value was set at 284.8 eV for correction. The N_2 physical adsorption/desorption isotherms were measured by Autosorb-iQA3200-4 sorption analyzer (Quantatech Co., USA). X-ray absorption spectroscopy (XAS) was tested on the 1W1B beamline of the Beijing Synchrotron Radiation Facility operated at 2.5 GeV and 200 mA. Thermogravimetric analysis (TGA) was performed on Discovery TGA550 with heating rate of $20^\circ \text{C min}^{-1}$ and temperature range from room temperature to 900°C . The UV-Vis spectra were acquired using a Shimadzu UV-2401 PC Recording Spectrophotometer. Ultraviolet photoelectron spectroscopy (UPS) analysis was conducted on ESCALAB 250xi with an unfiltered HeI (21.22 eV) gas discharge lamp at 2×10^{-8} mbar. All DFT calculations on N-confused porphyrin molecules in this study were performed using the Gaussian 09 program. The geometric optimization and electronic properties calculations of CMP-TPP, CMP-NCP, CMP-PtNCP and CMP-PtTPP were performed using the Vienna Ab-initio Simulation Package (VASP).

1.3 Synthesis of 5,10,15,20-tetrakis(4-bromophenyl) N-confused porphyrin (NCP4Br)

4-Bromobenzaldehyde (13.88 g, 75 mmol), freshly distilled pyrrole (5.2 mL, 75 mmol) and methanesulfonic acid (MSA, 3.89 mL, 60 mmol) were added into CH_2Cl_2 (1.5 L) in N_2 atmosphere and stirred for 30 minutes at room temperature. 2,3-dichloro-5,6-dicyanobenzoquinone (DDQ, 13.62 g, 60 mmol) was then added and stirred for 1 min. The reaction was then quenched by adding triethylamine (TEA, 24.9 mL, 180 mmol). The solution was purified by alkaline alumina column chromatography. The solvent polarity increased from 3:1 of n-hexane/ CH_2Cl_2 to 1:2, and finally to 100% CH_2Cl_2 . Finally, the green product was obtained as NCP4Br (3 g, 18%). $^1\text{H NMR}$ (CDCl_3 , 400 MHz): δ (ppm) 8.98-8.94 (dd, 2H), 8.76 (s, 1H), 8.64-8.55 (m, 4H), 8.25-8.19 (m, 2H), 8.06-

8.00 (m, 1H), 7.94-7.91 (m, 8H), -2.51 (s, 1H), -5.05 (s, 1H); ^{13}C NMR (CDCl_3 , 100 MHz): δ (ppm) 149.2, 147.1, 145.4, 140.8, 138.9, 135.8, 130.0, 124.4, 118.9; MALDI-TOF MS: calculated for $\text{C}_{44}\text{H}_{26}\text{Br}_4\text{N}_4$: 930.34, found: 930.44.

1.4 Synthesis of Pt(II) coordinated NCP4Br (PtNCP4Br)

PtCl_2 (136 mg, 0.51 mmol) was added into benzonitrile (10 mL), and then stirred for 12 hours at 130 °C. The solution was then distilled to obtain $\text{PtCl}_2(\text{PhCN})_2$. Then 1,2-dichlorobenzene (20 mL) and NCP4Br (100 mg, 0.1 mmol) was added in N_2 atmosphere and the mixture was stirred at 150 °C for 48 hours. After cooling, the solvent was removed by vacuum distillation. The crude product was purified by silica gel column with CH_2Cl_2 /hexane (4:1) as eluent. The dark brown solid was obtained as PtNCP4Br (20 mg, 17%). ^{13}C NMR (CDCl_3 , 100 MHz): δ (ppm) 140.8, 135.9, 134.5, 131.9, 130.6, 122.7, 118.3; MALDI-TOF MS: calculated for $\text{C}_{44}\text{H}_{24}\text{Br}_4\text{N}_4\text{Pt}$: 1123.4, found: 1123.81.

1.5 Synthesis of NCP4Br-derived conjugated microporous polymer (CMP-NCP)

1,5-cyclooctadiene (cod, 0.127 mL, 1.04 mmol), bis(1,5-cyclooctadiene) nickel ($\text{Ni}(\text{cod})_2$, 0.264 g, 0.96 mmol) and 2,2'-bipyridine (0.15 g, 0.96 mmol) were added into ultra-dry DMF (80 mL) and stirred at 80 °C for 40 minutes. NCP4Br (186.1 mg, 0.2 mmol) was dissolved in DMF (40 mL) and injected into the above purple solution. The mixture was stirred in N_2 atmosphere at 120 °C for 3 days. After cooling down, 400 mL of 1 M HCl was injected and continued to stir for 30 minutes. The precipitate was washed with chloroform, tetrahydrofuran and distilled water and dried in vacuum overnight to obtain CMP-NCP (83%). FTIR: (s-stretching, b-bending, w-wagging, r-rocking, def.-deformation) (cm^{-1}) 968 (C-C s in porphyrin), 1068 (C-H r), 1398 (C-C s + C-H r), 1642 (C=N s).

1.6 Synthesis of PtNCP4Br-derived conjugated microporous polymer (CMP-PtNCP)

Similar to operation 1.5, CMP-PtNCP was obtained by using PtNCP4Br as monomer in same steps. FTIR: (cm^{-1}) 1016 (N-H r), 1068 (C-H r), 1390 (C-C s and C-H r), 1642 (C=N s).

1.7 Synthesis of 5,10,15,20-tetrakis(4-bromophenyl) porphyrin (TPP4Br)

4-Bromobenzaldehyde (7.5 g, 40 mmol) was dissolved in a mixed solution of nitrobenzene (200 mL) and acetic acid (300 mL). Pyrrole (2.7 mL, 40 mmol) was added into the solution drop by drop under stirring. The solution was then stirred at 120 °C for 1 hour and cooled down to room temperature. The obtained atropurpureous sediment was washed by methanol (3×100 mL) and furtherly recrystallized with formaldehyde and chloroform to obtained TPP4Br (3.44 g, 34%). ^1H NMR (CDCl_3 , 400 MHz): δ (ppm) 8.87 (s, 8H), 8.09 (d, 8H), 7.93 (d, 8H), -2.85 (s, 2H). ^{13}C NMR (CDCl_3 , 100 MHz): δ (ppm) 140.8, 135.8, 130.0, 122.7, 119.0.

1.8 Synthesis of Pt(II) coordinated TPP4Br (PtTPP4Br)

$\text{PtCl}_2(\text{PhCN})_2$ was obtained as shown in operation 1.4. Then chloroform was added and refluxed for 2 hours together with sodium propionate (164 mg, 1.7 mmol) and TPP4Br (316 mg, 0.34 mmol). After the reaction, the product was poured directly onto a silica gel column and eluted with CHCl_3 . The eluent was collected and distilled to obtain the crude product. Acetonitrile and 2 drops of concentrated HCl was added, and the resulting suspension was stirred at 70 °C for 1 hour and then

cooled to room temperature. The brownish red sediment was washed with huge amounts of acetonitrile and dried overnight to obtain Pt-TPP4Br (31 mg, 69%). ¹H NMR (CDCl₃, 400 MHz): δ (ppm) 8.77 (s, 8H), 8.03 (d, 8H), 7.91 (d, 8H). ¹³C NMR (CDCl₃, 100 MHz): δ (ppm) 140.7, 140.0, 135.2, 130.8, 130.1, 122.7, 121.2.

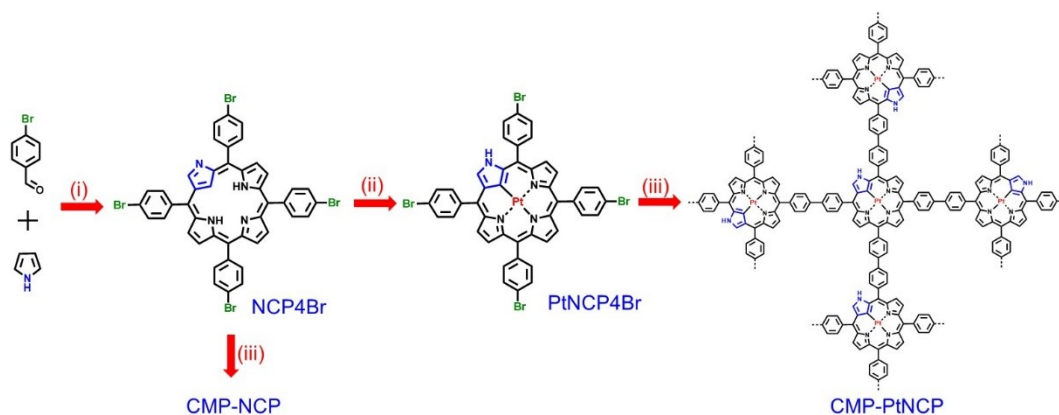
1.9 Synthesis of TPP4Br-derived CMP (CMP-TPP)

Similar to operation **1.5**, the CMP-TPP was obtained by using TPP4Br as monomer in same steps. FTIR: (cm⁻¹) 728/799 (N-H w), 843 (C-H w), 968 (C-C s in porphyrin), 1068 (C-H r), 1389 (C-C s and C-H r), 1640 (C=N s).

1.10 Synthesis of PtTPP4Br-derived CMP (CMP-PtTPP)

Similar to operation **1.5**, the CMP-PtTPP was obtained by using PtTPP4Br as monomer in same steps. FTIR: (cm⁻¹) 1068 (C-H r), 1389 (C-C s and C-H r), 1640 (C=N s).

2. Figures



Scheme S1 Synthesis routes of CMP-PtNCP and CMP-NCP. (i) methanesulfonic acid, RT, 30 min, and then DDQ, 8 min, and then TEA; (ii) [PtCl₂(PhCN)₂], 1,2-dichlorobenzene, reflux, 2 d; (iii) 1,5-cyclooctadiene (cod), bis(1,5-cyclooctadiene) nickel ([Ni(cod)₂]), 2,2'-bipyridyl, 80 °C, 3 d.

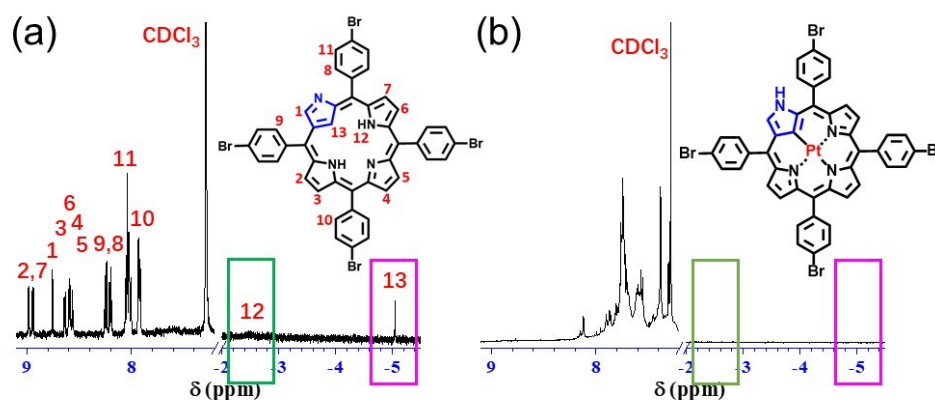


Fig. S1 ¹H NMR spectra of NCP4Br (a) and PtNCP4Br (b).

The δ of 12# and 13# H have disappeared, indicating that Pt(II) has been successfully coordinated with the N and C atoms.

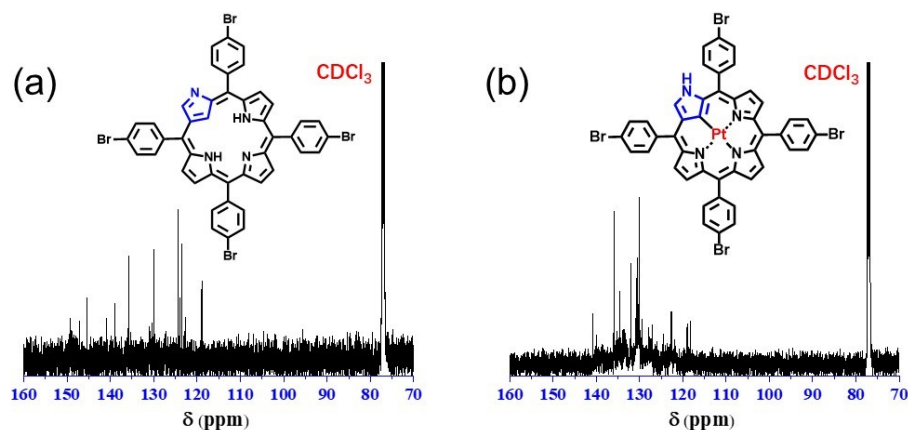


Fig. S2 ^{13}C NMR spectra of NCP4Br (a) and PtNCP4Br (b).

The chemical shifts δ (ppm) = 149.2, 147.1, 145.4, 140.8, 138.9, 135.8, 130.0, 124.4, 118.9 prove the structure of NCP4Br, while the chemical shifts δ (ppm) = 140.8, 135.9, 134.5, 131.9, 130.6, 122.7, 118.3 prove the structure of PtNCP4Br.¹

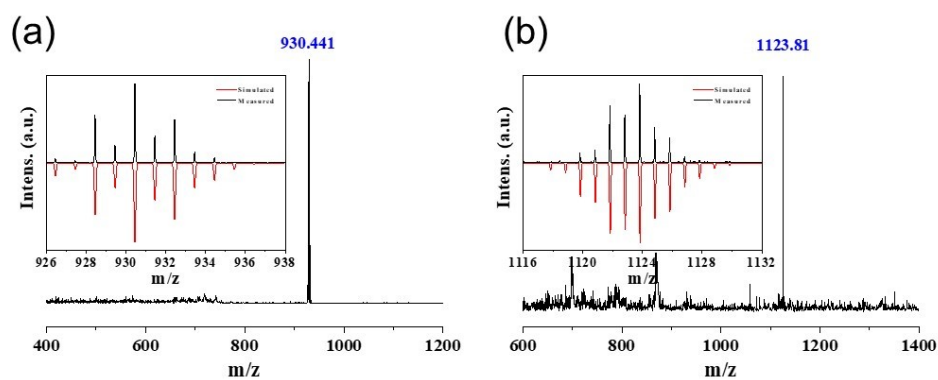


Fig. S3 Maldi-TOF MS spectra of NCP4Br (a) and PtNCP4Br (b), inset: HR-Maldi-TOF MS spectra.

Calculated for NCP4Br ($\text{C}_{44}\text{H}_{26}\text{Br}_4\text{N}_4$): 930.34, found: 930.44;

Calculated for PtNCP4Br ($\text{C}_{44}\text{H}_{24}\text{Br}_4\text{N}_4\text{Pt}$): 1123.4, found: 1123.81.

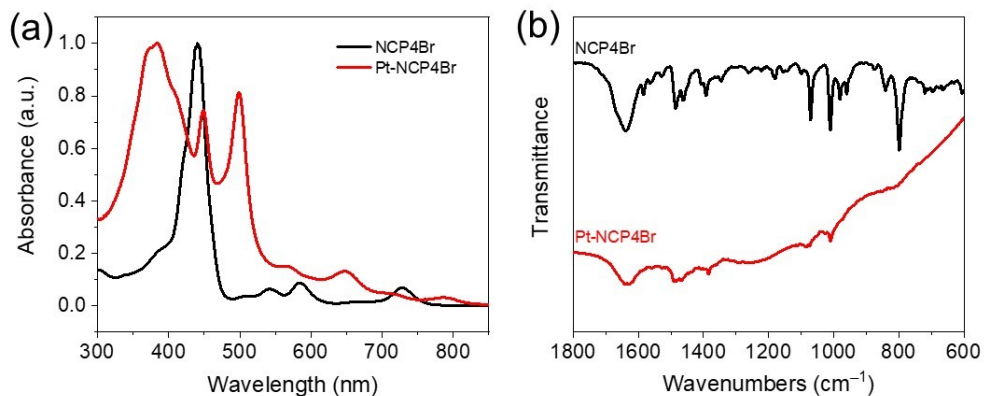


Fig. S4 UV-vis (a) and FTIR (b) spectra of NCP4Br and PtNCP4Br.

For UV-vis spectra, the maximum absorption wavelength of NCP4Br and PtNCP4Br are 442 and 382 nm, indicating that the conjugation degree of the system decreases after the introduction of metal Pt. For FTIR spectra, the peaks locate at 1072 and 723 cm^{-1} can be attributed to C-Br and C-H peak of pyrrole ring, while the disappearance of peak (N-H) at 967 cm^{-1} indicates that Pt is successfully coordinated with NCP4Br.

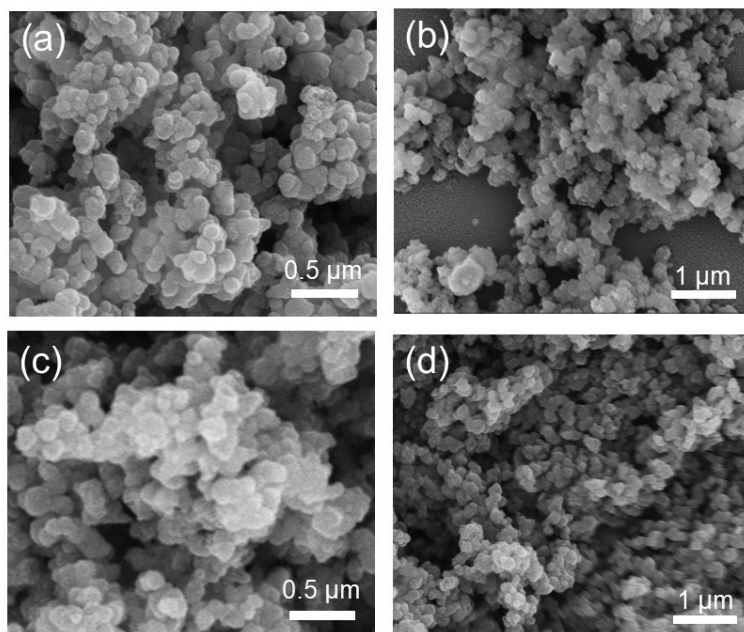


Fig. S5 SEM images of CMP-PtNCP (a), CMP-PtTPP (b), CMP-NCP (c) and CMP-TPP (d).

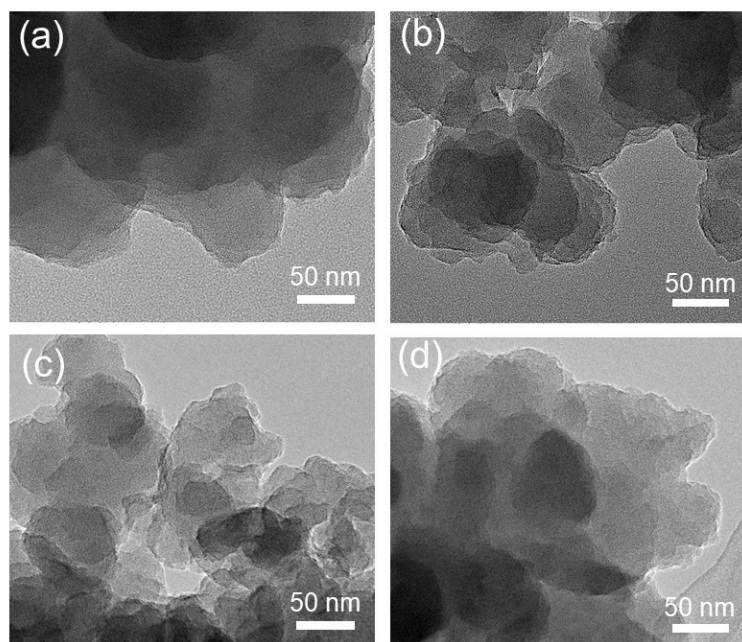


Fig. S6 TEM images of CMP-PtNCP (a), CMP-PtTPP (b), CMP-NCP (c) and CMP-TPP (d).

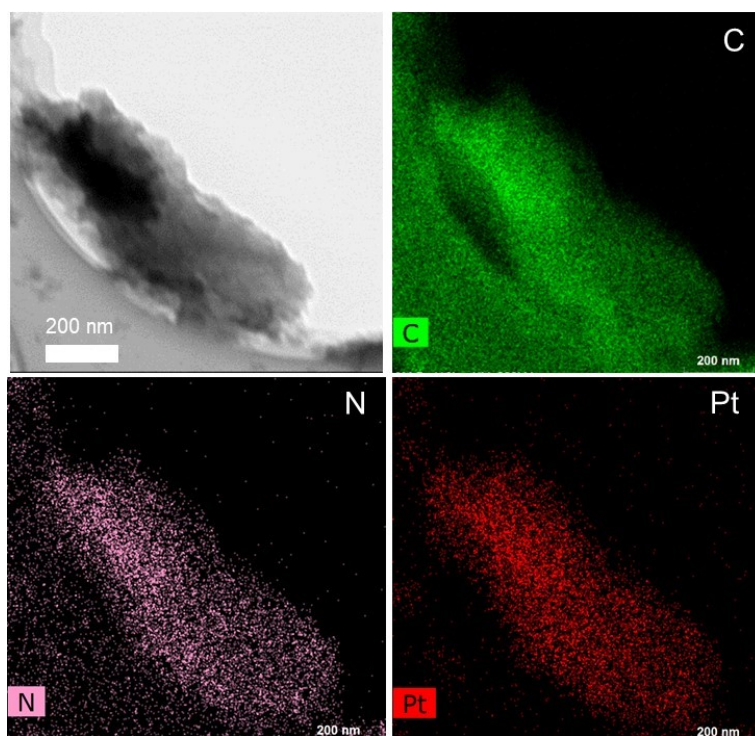


Fig. S7 STEM image and corresponding elemental mapping of CMP-PtNCP.

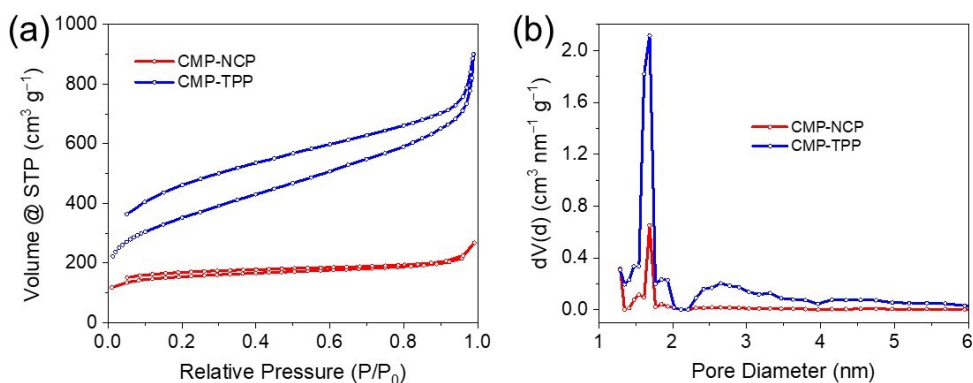


Fig. S8 N_2 adsorption-desorption isotherms (a) and pore size distribution (b) of CMP-NCP and CMP-TPP.

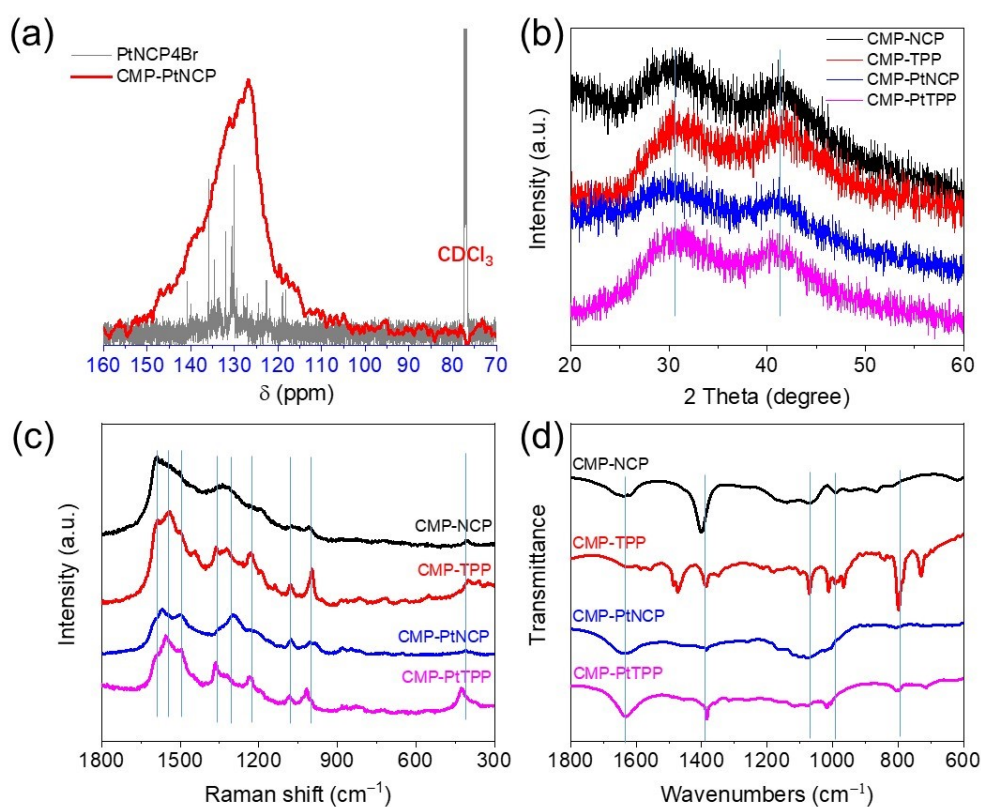


Fig. S9 (a) ^{13}C ssNMR spectrum of CMP-PtNCP. XRD patterns (b), Raman spectra (c), and FTIR spectra (d) of CMP-NCP, CMP-PtNCP, CMP-TPP, and CMP-PtTPP.

The phenylene linked carbon atoms are confirmed by peaks near 140, 130 and 122 ppm, while the signal of the porphyrin ring corresponds to the peak at 147 ppm,¹ as shown in (a). Raman spectra show that the characteristic peaks of the polymer are located at the Raman shifts of 426, 1018, 1084, 1236, 1363, 1497 and 1553 cm^{-1} , which is consistent with the reported materials based on metal

porphyrins². The FTIR spectra shows the C-Br peak at 1072 cm⁻¹, which can be ascribed to the end Br groups connected to the C atom of benzene rings.

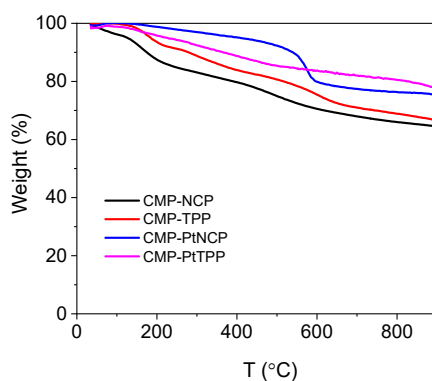


Fig. S10 TGA curves of CMP-NCP, CMP-PtNCP, CMP-TPP, and CMP-PtTPP.

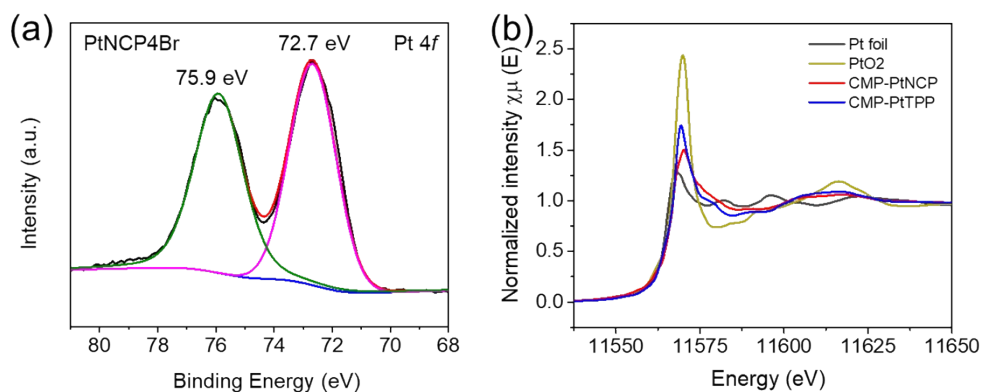


Fig. S11 (a) Pt 4f XPS spectrum of PtNCP4Br; (b) Pt L₃-edge XANES spectra of CMP-PtNCP and CMP-PtTPP.

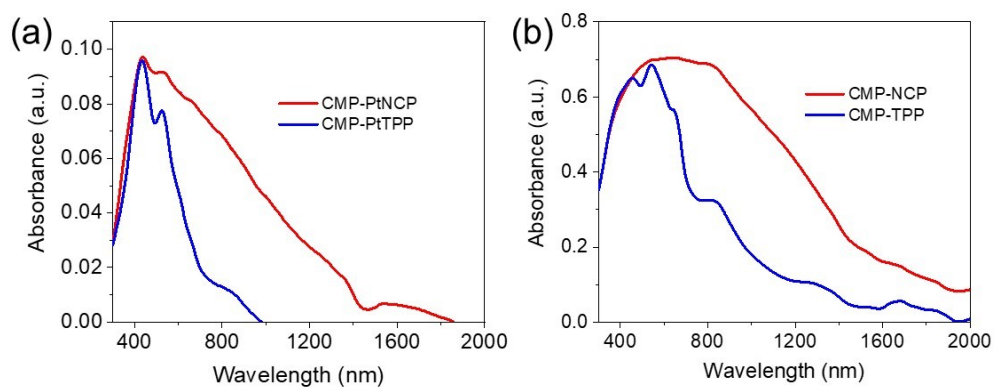


Fig. S12 UV-vis diffuse reflectance spectra of CMP-PtNCP, CMP-PtTPP, CMP-NCP and CMP-TPP.

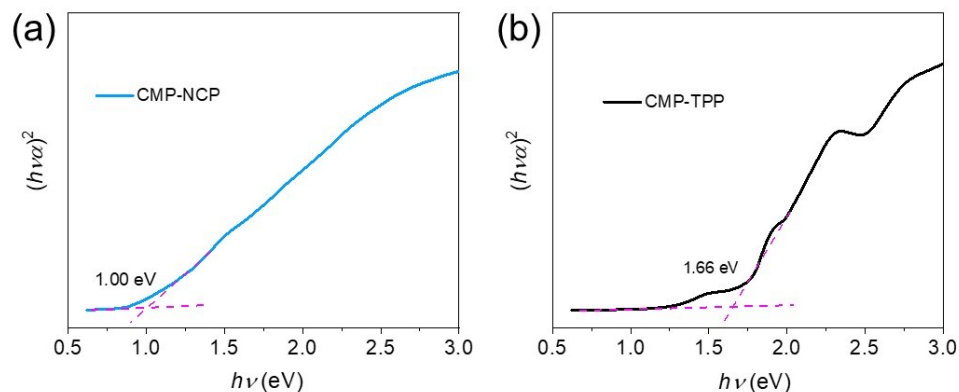


Fig. S13 T_{auc} plots for CMP-NCP (a) and CMP-TPP (b). The optical band gap of CMP-NCP and CMP-TPP are determined as 1.00 and 1.66 eV, according to KubelkaMunk (K-M) function.

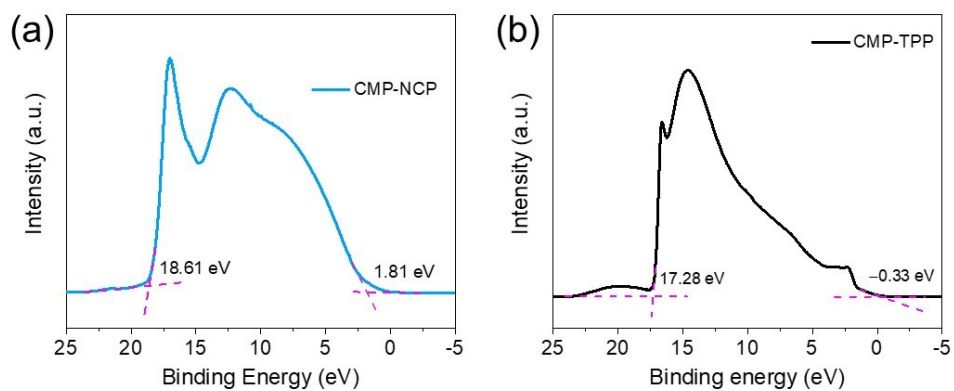


Fig. S14 UPS spectra for CMP-NCP (a) and CMP-TPP (b).

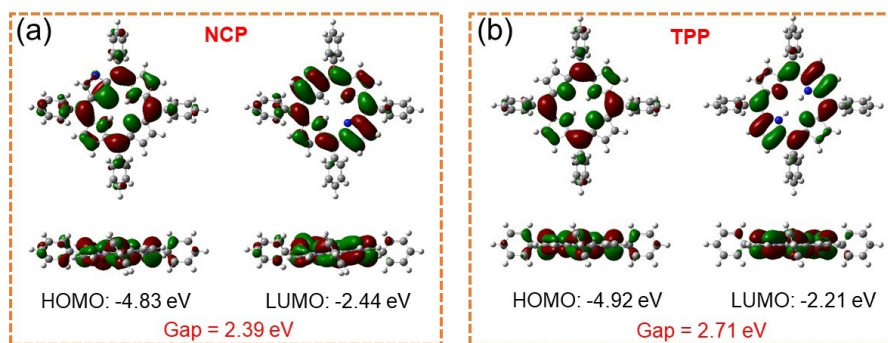


Fig. S15 The HOMO and LUMO levels of NCP (a) and TPP (b).

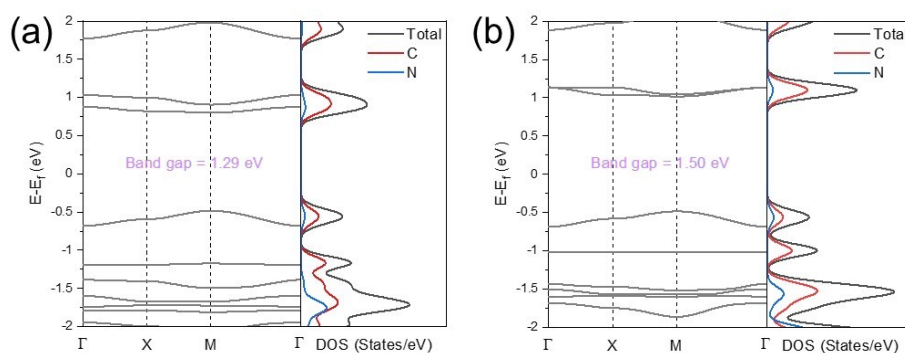


Fig. S16 Band structures and DOS of CMP-NCP (a) and CMP-TPP (b).

3. Table

Table 1 Textural parameters of the as-prepared CMPs based on nitrogen physisorption

Sample	S_{BET} ($\text{m}^2 \text{g}^{-1}$)	S_{micro} ($\text{m}^2 \text{g}^{-1}$)	V_{total} ($\text{cm}^3 \text{g}^{-1}$)	V_{micro} ($\text{cm}^3 \text{g}^{-1}$)	D (nm)
CMP-PtNCP	399	331	0.26	0.17	2.6
CMP-PtTPP	681	531	0.50	0.29	2.9
CMP-NCP	568	479	0.41	0.21	2.9
CMP-TPP	1257	561	1.39	0.27	4.4

4. references

1. Z.-S. Wu, L. Chen, J. Liu, K. Parvez, H. Liang, J. Shu, H. Sachdev, R. Graf, X. Feng and K. Müllen, *Adv. Mater.*, 2014, **26**, 1450-1455.
2. K. Lewandowska, N. Rosiak, A. Bogucki, J. Cielecka-Piontek, M. Mizera, W. Bednarski, M. Suchecki and K. Szaciłowski, *Molecules*, 2019, **24**, 688.